KINETIC APPROACH TO THE NO_X REDUCTION PROCESS BY POTASSIUM-CONTAINING COAL PELLETS UNDER OXYGEN-RICH MIXTURES.

A. Bueno-López[*] [a], J.A. Caballero-Suárez [b] and A. García-García [a].

[a] *Department of Inorganic Chemistry. University of Alicante. Spain.*
[b] *Department of Chemical Engineering. University of Alicante. Spain.*

[*]*Corresponding author (agus@ua.es).*

Introduction

Nitrogen oxides among other atmospheric pollutants are responsible of acid rain, photochemical smog and ozone layer depletion [1]. Therefore, NO_x emission abatement from combustion sources is a major objective for the incoming years. For this purpose, carbonaceous materials (coals, chars and active carbons) are effective under suitable operating conditions [2]. The use of carbon presents advantages with regard to gaseous reactants such the simplicity of the process, potentially lower cost and elimination of the environmental problematic "slip" of the gaseous reducing agent. In previous studies, our group reported promising results in terms of efficiency, selectivity towards NO_x against oxygen, selectivity towards the desired reaction products (N_2 versus N_2O and CO_2 versus CO) and long lifetimes by using potassium-containing coal briquettes and pellets [3,4].

In this study, we purpose the following four step kinetic model to describe to NO_x-carbon reaction, based on the general knowledge [5-7] and our own experience about the mechanism of this reaction [3,4,8,9].

$$C_f + O_2 \longrightarrow (CO)^{\#} \qquad (R1)$$

$$n_1 C + (CO)^{\#} \longrightarrow CO_2 + n_1 C_f \qquad (R2)$$

$$NO_x + C_f \longrightarrow 1/2 N_2 + (CO)^{\#} \qquad (R3)$$

$$n_2 C + NO_x + (CO)^{\#} \longrightarrow CO_2 + 1/2 N_2 + n_2 C_f \qquad (R4)$$

C_f makes reference to new freshly formed sites, created after the decomposition of oxygen-carbon groups through R2 or R4. These sites might be viewed as high reactive unsaturated atoms of carbon. $(CO)^{\#}$ includes all the oxygenated groups on the carbon surface that decomposes as CO_2 (via R2 or R4). The nature, stoichiometry and possible differences in relative stability of these groups are not fully known. C represents the carbon atoms different from C_f and $(CO)^{\#}$. It is important to note that CO_2 and N_2 are the only reaction products under the experimental conditions selected for this study [3]. Moreover, nitrogen balances pointed out that the formation of carbon-nitrogen complexes is not significant under our experimental conditions [8]. According to our

previous results, the water gas shift reaction and the carbon gasification by steam can also be rejected during experiments carried out including steam on the gas mixture [9].

The objectives of this study are (i) to prove the validity of this mechanism and (ii) to analyze the influence of the potassium catalyst, the reaction temperature and the presence of steam on the reaction pathway. To reach these objectives, the NO_x conversion and carbon consumption profiles during lifetime experiments were simulated by the Differential and Algebraic Equations system (DAE) deduced from the proposed mechanism. The set of kinetic parameters and the carbon active sites C_f and oxygen-carbon groups $(CO)^{\#}$ profiles predicted by the model will be discussed.

Experimental.

A Spanish high volatile A bituminous coal, (A3 with a 7.7% wt ash content), was used as coal precursor for this study. The commercial humic acid used to bind the powdered coal has a total humic extract of 16% w/w and the potassium content is 5% w/w. Four samples were prepared. The desired amounts of KOH were dissolved in humic acid using a fixed humic acid/coal ratio (1.2 ml/g of coal). The potassium-coal slurries were mixed for 30 min with stirring, dried at 110°C, and conformed in pellets (2 mm in diameter, average length of 8 mm). Finally, the pellets were pyrolyzed under N_2 for 2 h at 700°C. The samples were denoted by A3-K%, being "K%" the potassium weight percent after the pyrolysis step. The detailed method of coal-pellet preparation and their complete characterization were reported elsewhere [4].

The NO_x-carbon reduction tests were carried out at atmospheric pressure in a tubular quartz reactor (inner diameter = 1 cm). The reactor is coupled to a set of NDIR-UV specific gas analysers for NO, NO_2, CO, CO_2 and O_2. Isothermal reaction at several temperatures between 350 and 450ºC were performed under the reactive mixtures $0.2\%NO_x/5\%O_2/94.6\%N_2$ and $0.2\%NO_x/2\%H_2O/5\%O_2/92.8\%N_2$. The total reactive gas flow was 620 ml/min and 0.5 grams of pellets were used for each run, extended until complete carbon consumption.

The DEA system was solved by using the software ATHENA, version 8.3. This DEA includes three differential equations and two algebraic equations: $dC/dt = f(n_{1,2}, k_i, (CO)^{\#}, C_f, C)$; $dC_f/dt = f(n_{1,2}, k_i, (CO)^{\#}, C_f, C)$; $d(CO)^{\#}/dt = f(n_{1,2}, k_i, (CO)^{\#}, C)$, the mass balance of carbon species and the NO_x concentration, determined considering that the reactor behavior is like a *plug flow reactor* ($NO_x = f(NO_{x,0}, \tau, k_i, C_f, (CO)^{\#})$. In this equations: i=1,2,3,4; C_f, $(CO)^{\#}$ and C = mass fraction of active sites C_f, oxygen-carbon groups and carbon atoms different to C_f and $(CO)^{\#}$ respectively; NO_x=concentration of NO_x (mol/L); τ=residence time of gases on the solid bed (0.085 s).

The optimization algorithm used was the least square estimation:

$$O.F. = \min \sum_j \left[\left(mass_{exp}(t_j) - mass_{cal}(t_j) \right)^2 + \lambda \left(NO_{x\,exp}^{red}(t_j) - NO_{x\,cal}^{red}\left(t_j\right) \right)^2 \right] \qquad (1)$$

"j" makes reference to the experimental data (1 per hour), "mass" indicates the total mass fraction, the subscript "exp"' refers to experimental values and the subscript "cal" refers to calculated values. NO_x^{red} is the reduced NO_x. λ is a weight parameter introduced in order to force both terms in equation (1) to be of the same magnitude.

Results and discussion.

Table 1 summarizes all the lifetime tests performed and modeled (see reactive gas mixture, sample and temperature in the tittles of the columns). The total amounts of NO_x reduced during the experiments (g_{NO_x}/g_{sample}), the parameter "$S_{average}$" (average selectivity) and the eight adjusted parameters (four kinetic rate constants, the stoichiometric parameters n_1 and n_2 and the initial concentration of C_f and $(CO)^{\#}$) for all the lifetime experiments were included in Table 1. Further information about these experiments was reported elsewhere [4,9].

Table 1. Experimental results and adjusted parameters for the NO_x-carbon reduction process obtained by the simulation.

	$NO_x/O_2/N_2$						$NO_x/H_2O/O_2/N_2$	
Sample **Temperature**	**A3-7.9** **350ºC**	**A3-10.5** **350ºC**	**A3-16.8** **350ºC**	**A3-21.0** **350ºC**	**A3-16.8** **425ºC**	**A3-16.8** **450ºC**	**A3-16.8** **350ºC**	**A3-16.8** **450ºC**
$S_{average}$ (%)[(a)]	12	49	58	63	36	31	28	18
gNO_x/g_{sample}	0.5	1.9	2.0	1.8	1.3	1.2	1.0	0.7
k_1 (h^{-1})	1.24	1.18	1.72	2.44	6.00	8.10	6.00	34.00
k_2 (h^{-1})	0.082	0.039	0.061	0.121	0.190	0.239	0.110	0.350
k_3 ($l\ h^{-1}\ mol^{-1}$)	$0.03\cdot10^9$	$0.26\cdot10^9$	$0.59\cdot10^9$	$0.97\cdot10^9$	$0.75\cdot10^9$	$0.90\cdot10^9$	$0.30\cdot10^9$	$0.73\cdot10^9$
k_4 ($l\ h^{-1}\ mol^{-1}$)	$0.35\cdot10^9$	$0.45\cdot10^9$	$0.91\cdot10^9$	$2.12\cdot10^9$	$1.20\cdot10^9$	$1.29\cdot10^9$	$0.37\cdot10^9$	$1.00\cdot10^9$
n_1	4.36	4.28	3.88	3.46	4.50	4.60	3.20	3.23
n_2	1.00	2.00	2.93	2.63	1.50	1.53	2.01	1.46
$(CO)_0^{\#}$	0.082	0.049	0.021	0.002	0.040	0.082	0.050	0.105
Cf_0	0.005	0.014	0.002	0.001	0.003	0.006	0.002	0.002
V.C (%)[(b)]	4.33	3.36	1.79	2.86	4.47	3.50	0.79	0.91

[(a)] $S_{average} = \dfrac{(gNO_{x_{red.}}/NO_{molecular\ weight})}{(2\cdot(1\text{-}\%ash/100)/C_{atomic\ weight})}\cdot100$; $S_{average}$=100% → The carbon is only consumed by NO_x (desired reaction). $S_{average}$= 0% → The carbon is only consumed by O_2 (undesired reaction).

[(b)] The variation coefficient is a measure of the mathematical quality of the adjust [10]; $V.C(\%) = \sqrt{\dfrac{O.F.}{N-P}}\cdot100$ (being, O.F. the objective function (1), "N" the number of experimental values and "P" the number of adjustable parameters).

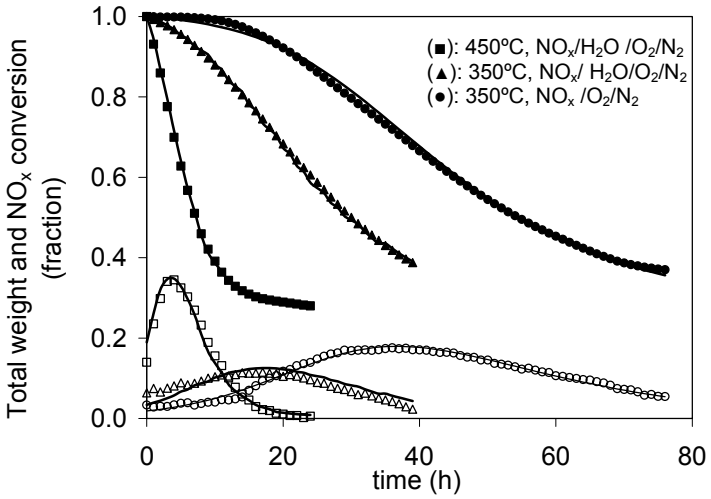

Figure 1. Total weight (solid symbols) and NO_x conversion (open symbols) profiles during selected lifetime tests with sample A3-16.8. Symbols: experimental data; lines: model fittings.

Figure 1 shows the NO_x conversion and sample consumption profiles for three selected experiments, including both the experimental data and the model fittings. It is important to note that the non-shown profiles are qualitatively similar, only presenting the expected differences on lifetime values, maximum NO_x conversions and so on. The simulation results on Figure 1 show good agreement with the experimental data, indicating that the proposed model describes successfully the reaction mechanism. Only important deviations were observed at the end of the lifetime tests, what means that the model fails in simulating the reaction data at very low carbon contents. For this reason, simulation profiles were only considered up to a certain reaction time, close to the end of the lifetime test.

The predicted C_f and $(CO)^{\#}$ profiles for the experiments on Figure 1 were included in the Figure 2. Simulation results predict that the C_f and $(CO)^{\#}$ concentrations follow similar behaviours, that is, both the C_f and $(CO)^{\#}$ concentrations increase with time until a maximum value is reached and then, the C_f and $(CO)^{\#}$ concentration decrease due to carbon consumption. These profiles are similar to those observed for NO_x conversion (see Figure 1). Note that the C_f appearance through the reaction is predicted to be very low if compared with the oxygen-carbon group profiles. This prediction is consistent with the idea that C_f species are highly reactive and short-life positions that will be quickly transformed to $(CO)^{\#}$, of much longer lifetime. It is generally accepted that the rate-limiting step in the range of temperatures used in this study is the low decomposition of the oxygen-carbon groups, in agreement with the profiles on Figure 2 [6].

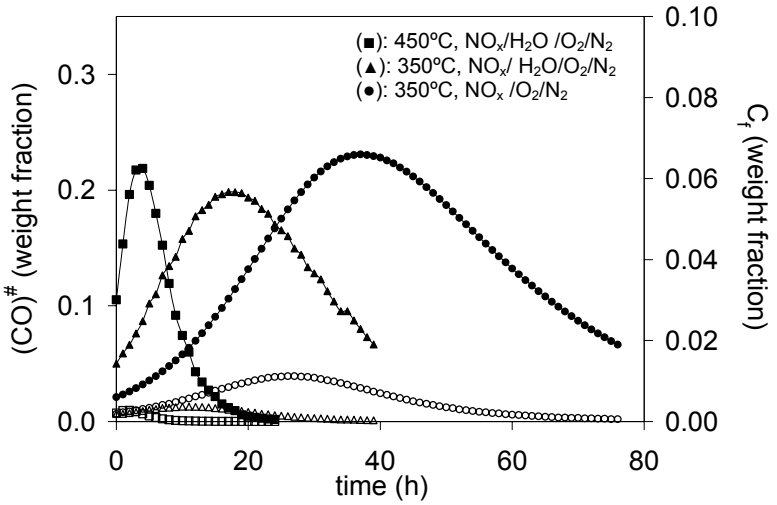

Figure 2. Predicted $(CO)^{\#}$ (solid symbols) and C_f (open symbols) profiles during selected lifetime tests with sample A3-16.8.

Data on Table 1 point out that all the rate constants k_i increase with temperature, as expected, both in the absence and presence of steam. Due to the corresponding units, only k_1 versus k_2 and k_3 versus k_4 are comparable in absolute values. For all the experiments, k_1 is one or two magnitude orders higher than k_2, what means that the oxygen chemisorption step R1 (via the catalyst or via direct attack to C_f positions) presents a higher rate constant value than that corresponding to the CO_2 evolution by direct decomposition of the oxygen-carbon groups (R2). These differences are also on line with the fact that the decomposition of oxygen-carbon groups is the rate-limiting step. On the other hand, k_3 and k_4 magnitude orders are almost similar.

In order to compare the four kinetic rate constants, k_i values were normalised and the corresponding dimensionless constants were plotted in Figure 3. Data on Figure 3a indicate that the temperature dependence of k_1 (oxygen chemisorption on active sites) and k_2 (oxygen-carbon groups decomposition) is much more important than the NO_x-involved steps dependence (steps R3 and R4). This finding is in agreement with the decrease in average selectivity towards NO_x with temperature. Normalised k_i values indicate that the higher the temperature, the higher the oxygen-carbon groups decomposition rate (k_2), as expected. The carbon reactivity increase due to C_f creation mainly favours the O_2 reaction, as deduced if $(k_1)_{normalised}$, $(k_3)_{normalised}$ and $(k_4)_{normalised}$ are compared.

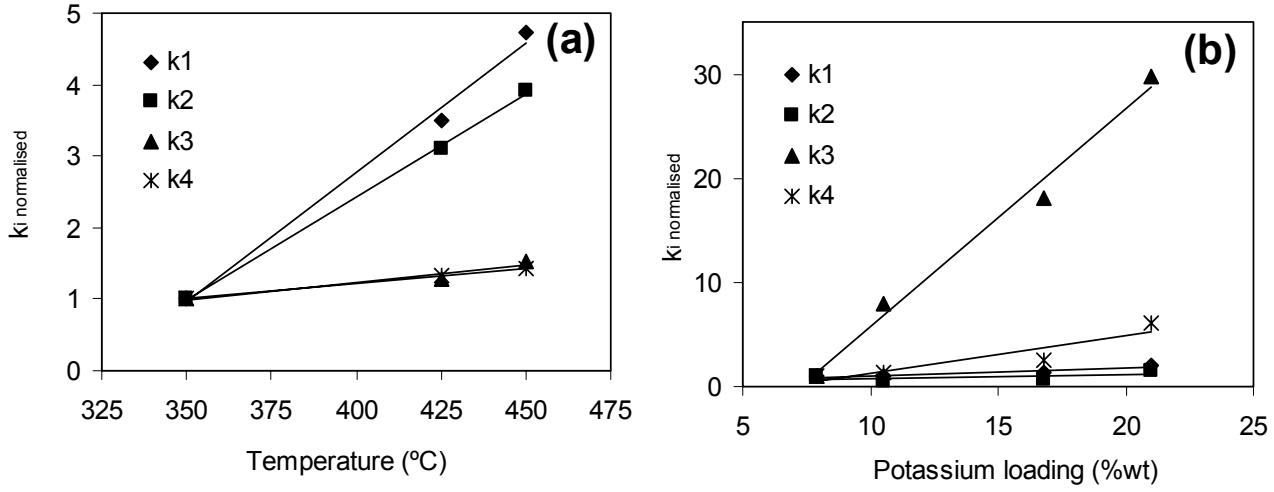

Figure 3 Normalised kinetic constants (reactive gas mixture $NO_x/O_2/N_2$).

(a) Sample: A3-16,8; T(ºC): 350, 425, 450; $k_{i\,norm.} = \frac{(k_i)_T}{(k_i)_{350ºC}}$; i=1,2,3,4.

(b) All the samples. T(ºC): 350; $k_{i\,norm.} = \frac{(k_i)_{A3-\%K}}{(k_i)_{A3-7.9}}$; i=1,2,3,4; %K=7.9, 10.5, 16.8, 21.0.

Data on Figure 3b points out that the potassium loading mainly affects the constant k_3, being the rest of constants less influenced. This issue could be the key to explain the high selectivity of this type of samples towards NO_x reduction against oxygen combustion. Note that the average selectivity towards NO_x increases with the potassium loading and reaches a maximum value of 63% for the highest potassium-loading sample (at 350ºC under $NO_x/O_2/N_2$). This value is very interesting considering that the O_2 level on the gas mixtures is 25 times higher than the NO_x concentration and, moreover, that O_2 is more reactive than NO [11] (NO is the main component of NO_x under our experimental conditions). Note also that, in spite of the sample A3-21.0 is the most selective one, the highest amount of NO_x is reduced by the sample A3-16.8 (compare gNO_x/g_{sample} for experiments at 350ºC under $NO_x/O_2/N_2$). This is due to the quite high ash content of the sample A3-21.0 (with a high loading of catalyst), and as a consequence of this, less carbon is available if compared with A3-16.8.

Regarding the steam influence on the rate constants, the comparison of data on Table 1 evidences that both k_1 and k_2 increase in the presence of steam, if constants at similar temperature and obtained with the same sample are compared. k_1 values in experiments under $NO_x/H_2O/O_2/N_2$ at 350 and 450°C are about four times higher than the counterpart constants under $NO_x/O_2/N_2$ and k_2 constants under $NO_x/H_2O/O_2/N_2$ are about 1.5 times higher that their counterpart under $NO_x/O_2/N_2$. On the contrary, the presence of steam on the gas mixture originates a slightly decrease of both k_3 and k_4 constants. These trends also explain the average selectivity decrease in the presence of

steam. Therefore, steam improves the $(CO)^{\#}$ decomposition via step R2 which mainly favors the O_2 attack to the nascent sites C_f via step R1. This finding confirms our hypothesis about the role of steam in this process, reported on reference [9]. Our previous results lead us to confirm that the presence of steam on the gas mixture favors the decomposition of some oxygen-carbon groups during the lifetime tests.

4. - Conclusions.

The four step kinetic model proposed in this study can successfully describe the NO_x reduction process by potassium-containing coal-pellets. The C_f and $(CO)^{\#}$ simulated profiles indicate that the rate-limiting step is the slow desorption of the relatively stable oxygen-carbon groups. Conversely, carbon active sites, C_f, present a shorter life.

The potassium loading mainly affects the kinetic rate constant of the NO_x chemisorption step (R3), thus explaining the increase in selectivity towards NO_x with the catalyst content exhibited by this type of samples. The reaction temperature mainly affects the kinetic rate constant of the oxygen-carbon groups decomposition (R2) and the O_2 chemisorption steps (R1), both under $NO_x/O_2/N_2$ and $NO_x/H_2O/O_2/N_2$, thus explaining the decrease of selectivity towards NO_x reduction with temperature. If data at similar temperature are compared, the kinetic rate constants of the surface complexes decomposition and the O_2 chemisorption steps (R2 and R1 respectively) increase in the presence of steam, supporting the hypothesis that H_2O acts as a destabilizing agent of the oxygen-carbon groups, thus improving the O_2 attack to the nascent sites on carbon surface.

References

[1] Loughurst J. W. S., Raper, D. W., Lee, D. S., Heath, B. A., King H. J. Acid deposition: a select review 1852–1990 : 1. Emissions, transport, deposition, effects on freshwater systems and forests. Fuel 1993; 72: 1261-1280.

[2] Tomita, A. Suppression of nitrogen oxides emission by carbonaceous reductants, Fuel Proc. Technol. 2001; 71: 53-70.

[3] Bueno-López A, Caballero-Suárez JA, García-García A. Analysis of the reaction conditions in the NO_x reduction process by carbon with a view to achieve high NO_x conversions. Residence time considerations. Energy Fuels 2002;16:1425-1428.

[4] Bueno-López A, García-García A, Caballero- Suárez, JA, Linares Solano A. Influence of potassium loading at different reaction temperatures on the NO_x reduction process by potassium-containing coal pellets. Fuel 2003; 82:267-274.

[5] Illán Gómez MJ, Linares Solano A, Radovic LR, Salinas Martinez de Lecea C. NO reduction by activated Carbons. 7. Mechanistic Aspects of Uncatalyzed and Catalyzed Reaction. Energy Fuels 1996;10:158-168

[6] Aarna I., Suuberg M. A review of the kinetics of the nitric-oxide-carbon reaction. Fuel 1997;76,6:475-491.

[7] Li Y.H., Lu G.Q., Rudolph V. The kinetics of NO and N_2O reduction over coal chars in fluidised bed combustion. Chem.Eng. Sci. 1998;53,1:1-26.

[8] García-García A.; Illán-Gómez M.J.; Linares-Solano A.; Salinas-Martínez de Lecea C. Thermal treatment effect on NO reduction by potassium-containing coal-briquettes and coal-chars. *Fuel Proc. Tech.* 1999, *61*, 289-297.
[9] Bueno-López A. and García-García A. Potassium-containing coal pellets for NO_x reduction under gas mixtures of different composition. Carbon 2004, accepted.
[10] Himmelblau, D.M.. *Process Analysis Statistical Methods,* Wiley: New York, 1970.
[11] García García A, Illán Gómez MJ, Linares Solano A, Salinas Martínez de Lecea C. NO_x reduction by Potassium-Containing Coal Briquettes. Effect of NO_2 Concentration. Energy Fuels 1999; 13: 499-505.